

Differential Processing of Objects under Various Viewing Conditions in the Human Lateral Occipital Complex

Kalanit Grill-Spector,* Tammar Kushnir,[†]
Shimon Edelman,[§] Galia Avidan,[‡] Yacov Itzhak,[†]
and Rafael Malach^{*||}

*Weizmann Institute of Science
Rehovot 76100

[†]Diagnostic Imaging Department
The Chaim Sheba Medical Center
Tel Hashomer 52621

[‡]Hebrew University
Jerusalem 91904
Israel

[§]Department of Psychology
Cornell University
Ithaca, New York 14850

Summary

The invariant properties of human cortical neurons cannot be studied directly by fMRI due to its limited spatial resolution. Here, we circumvented this limitation by using fMR adaptation, namely, reduction of the fMR signal due to repeated presentation of identical images. Object-selective regions (lateral occipital complex [LOC]) showed a monotonic signal decrease as repetition frequency increased. The invariant properties of fMR adaptation were studied by presenting the same object in different viewing conditions. LOC exhibited stronger fMR adaptation to changes in size and position (more invariance) compared to illumination and viewpoint. The effect revealed two putative subdivisions within LOC: caudal-dorsal (LO), which exhibited substantial recovery from adaptation under all transformations, and posterior fusiform (PF/LOa), which displayed stronger adaptation. This study demonstrates the utility of fMR adaptation for revealing functional characteristics of neurons in fMRI studies.

Introduction

A large cortical expanse located on the lateral and ventral aspects of the occipital lobe is activated preferentially by images of objects, including faces, as compared to a wide variety of textures and visual noise patterns. This region is situated laterally to the retinotopically organized areas V4/V8 (Sereno et al., 1994; DeYoe et al., 1996; Tootell et al., 1996; Hadjikhani et al., 1998) and was termed the lateral occipital complex (LOC) (Malach et al., 1995; Grill-Spector et al., 1998a, 1998b; see also Kanwisher et al., 1996).

Functionally, several characteristics of the LOC indicate homologies with macaque IT cortex (Malach et al., 1995; Tootell et al., 1996). Particularly intriguing is the finding that the amplitude of LOC activation remains constant despite changes of up to 4-fold in stimulus

size (Malach et al., 1995), as well as changes in stimulus location within the visual field (Grill-Spector et al., 1998b; Tootell et al., 1998c). These response properties are in line with the presumed role of the LOC in object recognition (Malach et al., 1995), a behavioral task that requires position and size invariance (Edelman, 1997), and are also compatible with the large receptive fields of macaque IT neurons, which show substantial size invariance (Gross et al., 1972; Desimone et al., 1984; Ito et al., 1995).

However, care should be exercised in interpreting the results of fMRI mapping. The limited spatial resolution of fMRI (3–6 mm) may average out a heterogeneous group of highly selective neurons. For example, the overall activity of a mixture of neuronal populations, each tuned to a different object size during object size changes, may produce a steady fMRI signal, creating a deceptive impression of size invariant behavior. A similar argument can be invoked to challenge the lack of retinotopy within the LOC.

This problem of averaging may be circumvented by using stimulus repetition effects. Recently, it has been reported that high-order human visual areas show a reduction in the fMR signal when presented repetitively with the same visual stimulus (Martin et al., 1995; Stern et al., 1996; Buckner et al., 1998; Tootell et al., 1998b; and see the review by Wiggs and Martin, 1998). A similar phenomenon was also reported for repetitively presented words (Buckner et al., 1995) and as the initial phase in procedural motor learning (Karni et al., 1995). It was suggested that this effect is correlated to visual priming (Biederman and Cooper, 1991; Buckner et al., 1998; Schacter and Buckner, 1998; Wiggs and Martin, 1998), although a direct link between these phenomena has not been demonstrated yet.

The neuronal mechanisms underlying the repetition effect are not clear at this stage, but a straightforward interpretation is neuronal adaptation. Indeed, shape adaptation has been documented by several studies in macaque IT neurons (Rolls et al., 1989; Miller et al., 1991; Li et al., 1993; Sobotka and Ringo, 1993). Lacking direct single unit recordings from the LO complex (LOC), we will tentatively refer to the measured fMRI signal reduction as functional magnetic resonance adaptation (fMR-A).

The application of fMR-A to study the functional properties of cortical neurons proceeds in two stages. First, the neuronal population is adapted by a repeated presentation of a single stimulus. Second, some property of the stimulus (e.g., size, translation, illumination, or viewpoint) is varied, and the recovery from adaptation is assessed. Consider, for example, the issue of size selectivity. If LOC neurons are size invariant, then rescaling the stimulus will produce adaptation, as they are essentially “blind” to this manipulation. If, however, LOC contains a mixture of neuronal groups each tuned to a different optimal object size, then for each stimulus size presented, a new group of neurons will be activated. Therefore, these neurons would not be adapted, and the result will be a strong fMRI signal (i.e., a recovery

|| To whom correspondence should be addressed (e-mail: bnmalach@wis.weizmann.ac.il).

from the adapted state). Thus, fMR-A can help in revealing the invariant properties of neuronal groups.

In the present experiments, we first characterized fMR-A in terms of its anatomical localization and duration. We then used fMR-A to investigate size, translation, illumination, and rotation invariance of LOC neurons. Our results show that LOC voxels are less sensitive to changes in stimulus size and position compared to changes induced by illumination and viewpoint. Moreover, the adaptation effect revealed subdivisions within the LOC: the anterior–ventral portion of the LOC was located in the posterior fusiform (PF/LOa; Halgren et al., 1999). It showed translation and size invariant adaptation, while the caudal–dorsal subdivision (LO) showed a substantial recovery from adaptation under all object transformations. These results show that fMR-A can provide a powerful tool for assessing the functional properties of cortical neurons. Some of these results have been published previously in an abstract form (Grill-Spector et al., 1998c; Malach et al., 1998).

Results

The Adaptation-Duration Experiment

Before attempting to use fMR-A to study invariances of object representation, it was essential to establish the magnitude and duration of this effect and its anatomical localization. To that end, we performed the adaptation-duration experiment in nine subjects (see the Experimental Procedures). In this experiment, cycles containing different visual objects were repeated over the length of the epoch. Object epochs differed in the number of different objects presented in the repeating cycle from one object image presented repeatedly (epoch 1) to 32 different object images (epoch 32; see Figure 1) presented once.

To localize object-selective areas and compare them to primary visual areas, we conducted two independent statistical tests. One test searched for voxels activated preferentially during the object epochs compared to the visual noise epochs (linear regression, object > noise and blanks). This contrast has been shown previously (Malach et al., 1995; Grill-Spector et al., 1998a, 1998b) to delineate reliably high-order object-related areas, particularly the LOC. The other test searched for voxels activated preferentially during the noise epochs compared to object epochs. This test has been shown previously (Grill-Spector et al., 1998a) to reveal primary visual areas (linear regression, noise > objects and blanks).

As expected, the two tests highlighted different sets of visual areas, as shown in Figure 2a for three different subjects. Note that medial occipital areas were activated preferentially by visual noise patterns, while lateral areas were preferentially activated by images of objects. A comparison between these maps and the borders of retinotopic visual areas (Sereno et al., 1994) as defined by the vertical and horizontal meridian mappings (see the Experimental Procedures and Figure 2b) indicated that the medial areas activated preferentially by visual noise corresponded to areas V1 and V2 with occasional invasion into VP.

The object-selective areas included several distinct foci. A large and weakly retinotopic region, situated on the lateral–ventral aspect of the occipital lobe, was termed the LOC (Malach et al., 1995; Grill-Spector et al., 1998a). A small dorsal focus of activation was evident in five out of nine subjects and appeared to overlap area V3a or an area anterior to it (Grill-Spector et al., 1998a). Finally, a small ventrolateral region of overlap of retinotopic regions and object-selective activation (yellow patch in Figure 2b) was located medial to LOC and appears to correspond to areas V4/V8.

The functional profiles of the object-selective and visual noise-activated regions revealed a markedly different behavior. Figure 3 summarizes these differences by showing data averaged from nine subjects. Note that object-selective areas (Figure 3b) showed a reduced activation when the same objects were repeated, particularly in the epochs containing only one or two objects (epochs 1 and 2). The activation level in these epochs was decreased compared to the level of activation in the epoch containing 32 different images (epoch 32). In contrast, primary visual areas that showed preferential activation to visual noise patterns (Figure 3a) showed similar activation levels in the different repetition cycles (i.e., these areas remained essentially unadapted under the specific conditions of this experiment [compare 1 and 32, Figure 3a]). Note, however, that the object stimuli used were suboptimal for V1 activation, which may account for the lack of adaptation.

Using meridian mapping, we analyzed separately the activation profiles of LOC (Figure 3c) and area V4 (Figure 3d). V4 was located ventrally, adjacent to the second upper vertical meridian representation (see Figure 2b, yellow patch). LOC voxels were lateral and anterior–ventral to retinotopic regions. The results showed fairly similar activation profiles with a somewhat reduced adaptation level in V4 (but stronger absolute signal, especially in the noise and texture epochs) compared to LOC. Thus, in LOC, the fMRI signal for the epoch with maximal number of repetitions (epoch 1) was $48\% \pm 4\%$ (SEM) of the nonrepeating (epoch 32) activation, while in V4 it was $56\% \pm 4\%$ (SEM). This somewhat weaker effect in V4 is compatible with our previous results (Grill-Spector et al., 1998b) that placed V4 functionally between LOC and the primary visual areas. As is apparent in a comparison of Figure 3b to Figure 3c, LOC activation was very similar to the overall behavior of object-selective regions defined by the statistical test (objects > noise). This is due to the unequal size of area V4 and LOC; the number of voxels that were unambiguously confined to V4 was 35 ± 14 SD (standard deviation) in both hemispheres, while the number of LOC voxels was 225 ± 138 SD (both hemispheres).

An issue of interest is how the fMR-A is affected by the repetition frequency (i.e., by the time elapsing between object repetitions). To quantitate this effect, we analyzed the level of activation in the second half of each object epoch by calculating the adaptation ratio (see the Experimental Procedures) compared to the maximal activation (epoch 32) just for this part of the epoch. The second half of each epoch was chosen because at least two repetition cycles elapsed prior to it even in the epoch containing the longest (eight pictures) repeating cycle.

The results of this analysis are shown in Figure 3e.

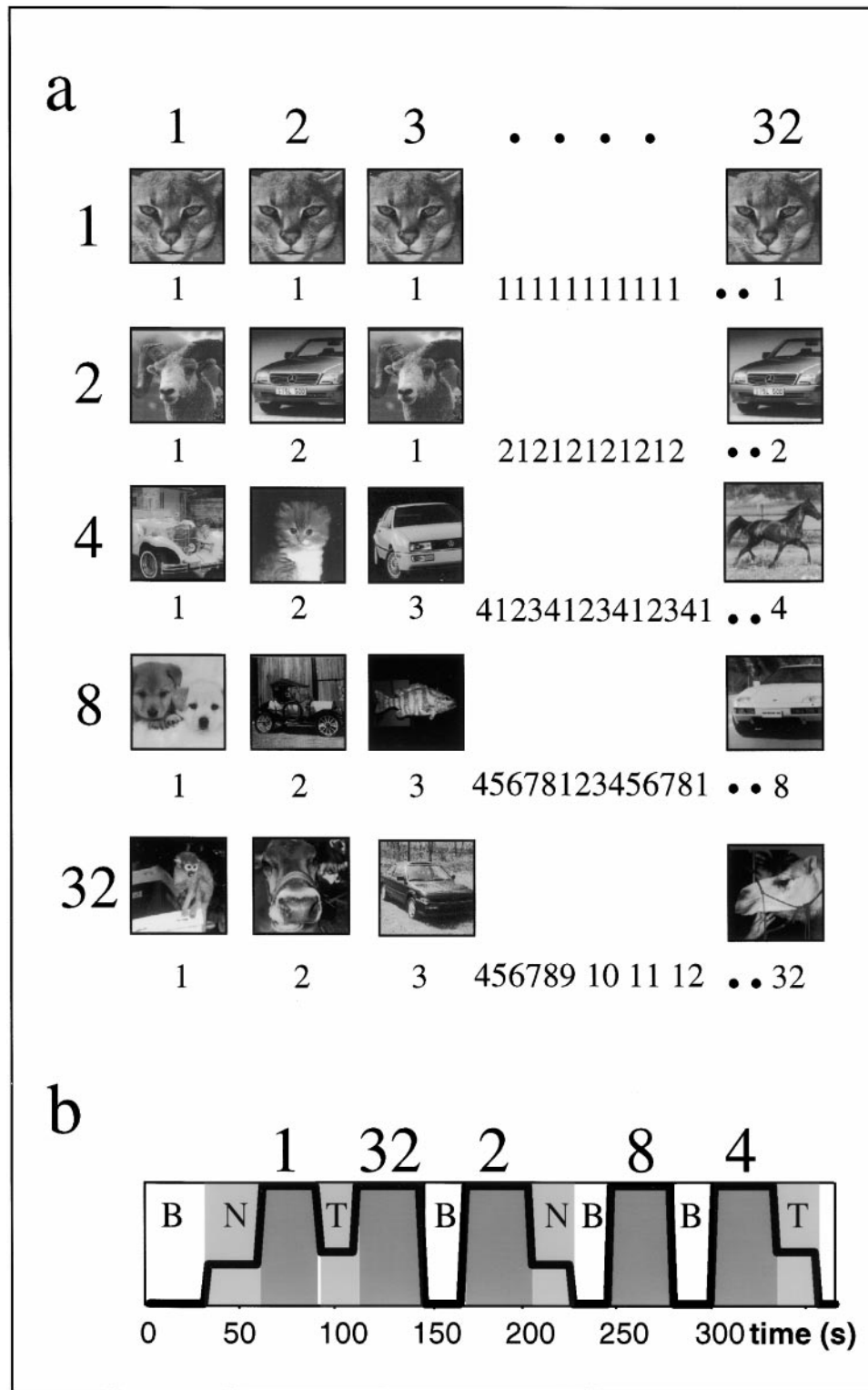


Figure 1. The Adaptation-Duration Experiment

(a) An illustration of the sequence of object images presented during the adaptation-duration experiment (see the Experimental Procedures). The number of different objects in each repeating cycle is given on the left, ranging from the same object picture presented repeatedly (1) to 32 different images (32).

(b) The time sequence of epochs in the experiment. Object epochs alternated with either texture patterns (T), highly scrambled images (N), or mean luminance blank field (B). Thick black line indicates object epochs (full amplitude), noise/textured epochs (middle amplitude), and blank field (baseline).

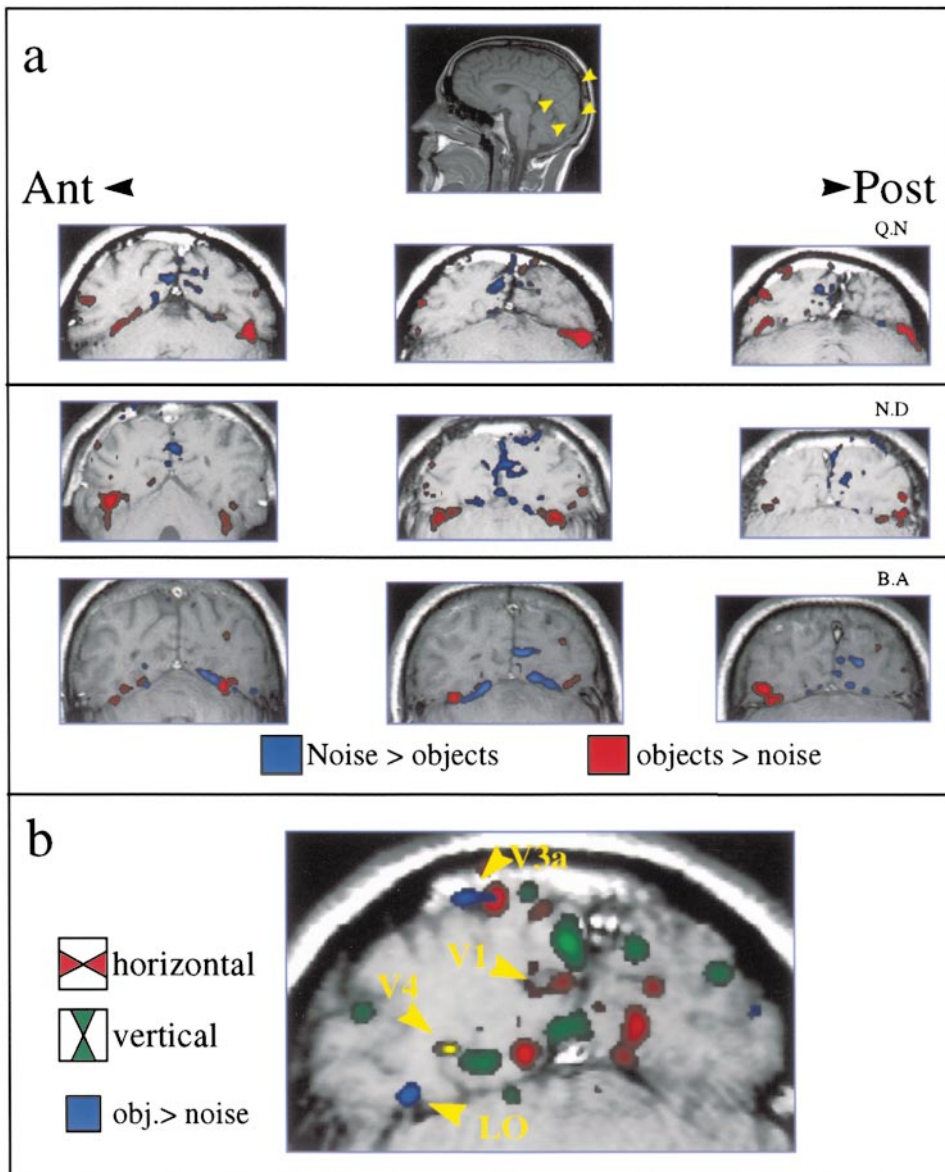


Figure 2. Adaptation-Duration Experiment: Localization of Object- and Texture-Related Regions

(a) Three consecutive oblique sections taken from three subjects. The approximate orientation and range of the sections is given in top plate. Areas colored in blue indicate regions in which activity was significantly ($p < 0.001$) higher for noise compared to objects (test: regression to an ideal boxcar time course: texture and noise $>$ objects and blanks). Red indicates regions in which activity was significantly higher ($p < 0.001$) for object versus noise (test: regression to an ideal time course: objects $>$ texture and noise and blanks). Color brightness indicates level of significance. Note that blue regions are located in medial regions while red regions are located laterally.

(b) Relationship of object-related regions and meridian mapping. Horizontal (HM) and vertical (VM) meridian representations (red and green, respectively) are superposed on object-related regions revealed by the object test as in (a). Area V4 (yellow patch) showed overlap of object selectivity and retinotopy. The essentially nonretinotopic LO complex (blue) was located more laterally.

When the same object picture was shown repeatedly, signal strength in LOC was reduced at the second half of the epoch to $42\% \pm 6\%$ (SEM) of the activation in the no repetition epoch (32). Signal amplitude increased monotonically as the repetition frequency decreased and the cycle of different pictures increased (along with the separation between repetitions). Note that even in the eight picture cycle, with 8 s separating between repetitions, there was a slight reduction in signal strength ($92\% \pm 5\%$). To obtain a quantitative estimate of the correlation between cycle length and adaptation level, we calculated a linear regression between the fMR-A level and the number of different images per

cycle. This was done for each subject for cycles containing one to eight pictures. The slope of the linear regression was $7.16\% \pm 0.69\%$ (percent increase per image) and was highly significant ($p < 10^{-6}$).

The Size Invariance Experiment

Having established that fMR adaptation is a consistent and fairly long lasting effect, we used fMR-A to explore size invariance in seven subjects (see Figure 4a and the Experimental Procedures for details). If LOC response is size invariant, voxels that are adapted by size changes should be activated equally by small and large objects.

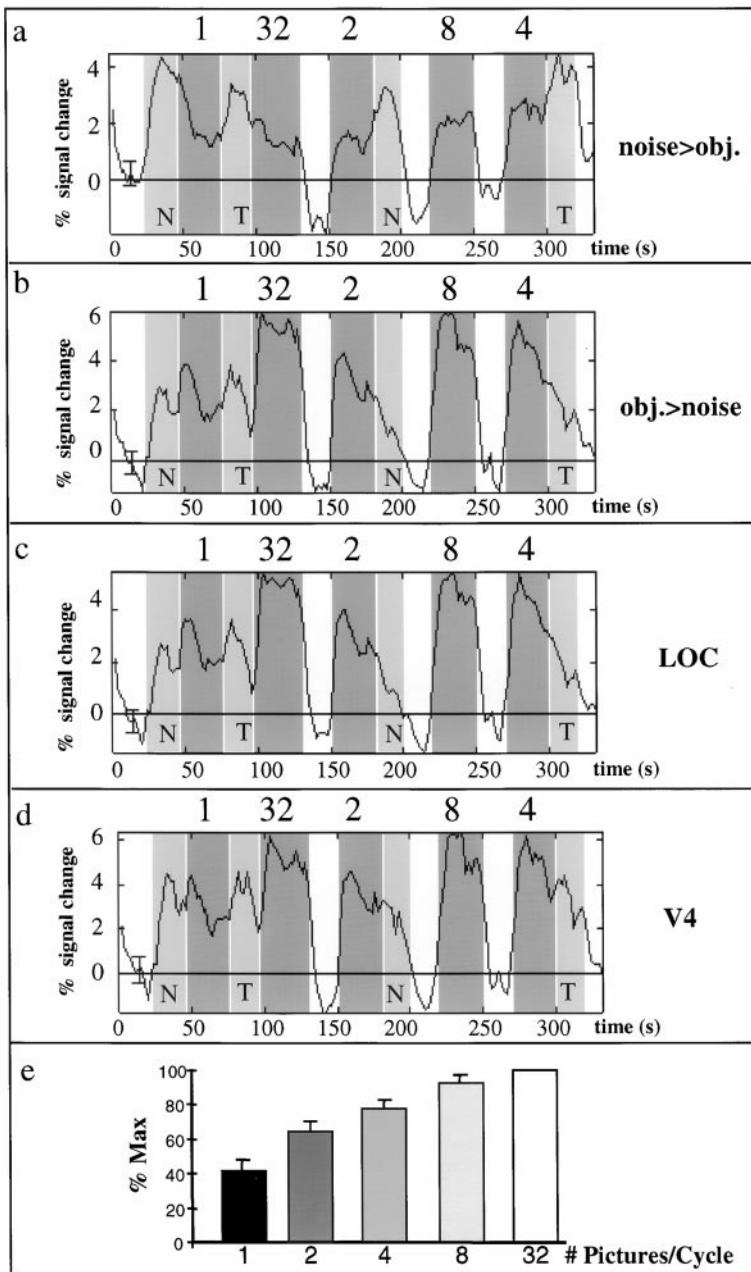


Figure 3. Adaptation-Duration Experiment: Activation Time Courses

Averaged time course data from nine subjects. The percent signal change from a blank baseline is plotted against time. Error bars show average ± 1 SEM. Shaded regions indicate epochs in which pictures were displayed. Object epochs are illustrated (see Figure 1a) by the dark shaded bars; the numbers on top indicate the number of different images presented in each epoch. Nonobject stimuli are indicated inside the light gray bars (T, textures; N, scrambled images).

(a) Medial regions activated preferentially by visual noise compared to objects (blue in Figure 2a).

(b) Lateral regions activated preferentially by objects compared to noise patterns (red in Figure 2a).

(c) LO complex (LOC) as defined by the meridian mapping experiments (blue in Figure 2b).

(d) V4 as defined by the meridian mapping experiments (yellow in Figure 2b).

(e) Relative LOC signal in the second half of each object epoch compared to the maximal activation (epoch 32) as a function of number of different pictures in the cycle. Note the monotonic decrease in the fMRI signal as the repetition frequency is increased.

To test this prediction, we compared the level of activation for large and small line drawing stimuli as well as the degree of fMR-A to changes in object size.

Another issue examined in this experiment was the dependence of the fMR-A on shape category. It could be argued that the observed adaptation was not related to the object's shape, but rather to its semantic category (i.e., subjects covertly repeated the same object name during the adaptation period). To test for that possibility, we included an epoch (Semantic control) containing different exemplars of the same semantic category (dogs).

We ran a statistical test searching for voxels activated preferentially by objects compared to noise and texture patterns, while the repeated object (Identical) and different object sizes (Size) epochs were not considered in the statistical analysis (Kolmogorov-Smirnov statistical

test: Semantic control and Small and Large > Noise and Texture). Similar to the previous experiment, this test highlighted more lateral foci, corresponding in anatomical location to LOC with a small, occasional dorsal focus (Figure 4b). The activation profile averaged across seven subjects is shown in Figure 4c.

It is quite clear from Figure 4c that activation to small and large objects was similar. The onset of the adaptation in this experiment was more gradual (i.e., the adaptation did not occur immediately). The adaptation ratio in the "identical" epoch was 0.71 ± 0.05 (SEM) of "large" and "small" shape activation (a ratio of 1.0 corresponds to no adaptation). A statistical test revealed that the adaptation effect was significant ($p < 0.002$, t test). Adaptation remained when object size was changed (size adaptation ratio, 0.56 ± 0.06 of "large" and "small"

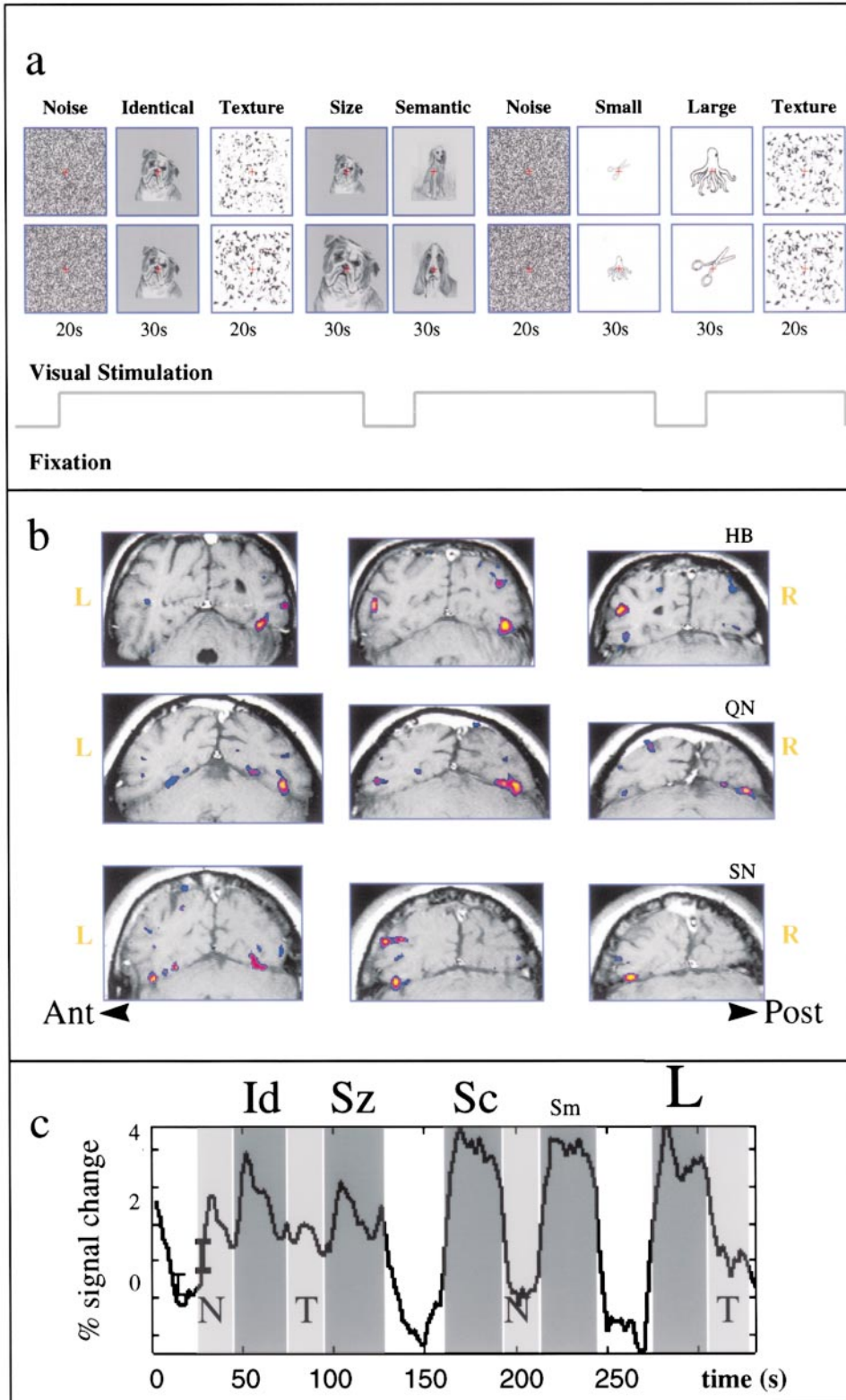


Figure 4. Size Invariance Experiment

(a) Examples of images from each epoch (see the Experimental Procedures). Noise (N), random dot patterns; Identical (Id), same drawing shown repeatedly; Texture (T), random triangles; Size (Sz), same as Id but presented in 30 different sizes over a 2-fold range; Semantic control (Sc), 30 drawings of different dogs; Small (Sm), 30 different common objects (size, $7^{\circ} \times 7^{\circ}$), Large (L), same as Sm but reordered (size, $22^{\circ} \times 22^{\circ}$). (b) Three consecutive oblique sections taken from three subjects. Same conventions as in Figure 2a. Cortical regions significantly ($p < 10^{-7}$; blue, $p < 10^{-4}$) activated by objects compared to noise (see [a]) were defined by a Kolmogorov-Smirnov statistical test: Lg and Sm and Sc > N and T; Identical and Size epochs not considered. Ant, anterior; Post, posterior; R, right; L, left.

epochs). This effect was highly significant ($p < 0.0002$, t test).

Overall, there was no apparent adaptation effect when different object shapes were limited to the same semantic category (semantic control adaptation ratio, 1.06 ± 0.07 , of large and small epochs). However, since LOC is a complex region, we were interested to see if it contained subregions that nevertheless showed a semantic adaptation effect (i.e., a significantly reduced signal when exemplars of the same semantic category were presented). A voxel by voxel analysis indeed revealed a small population of such voxels ($4.8\% \pm 4.5\%$, SD of the entire LOC). However, they were quite variable between subjects both in their extent and in their anatomical location within the LOC.

In contrast to LOC, most voxels in primary visual areas that showed preferential activation to visual noise or textures (data not shown) exhibited a marked signal increase during the large objects epoch compared to the small objects epoch. Most likely, this is a consequence of the larger retinotopic extent of the larger objects, which produces a wider expanse of activation in retinotopic visual areas.

Comparison of Various Object Transformations

Face Experiment 1: Translation-Illumination-Rotation Invariance

To compare the sensitivity of fMR-A to changes in object position, illumination, and rotation, we used two semantic categories of stimuli: faces and cars. Activation to identical objects undergoing these changes was compared to different objects in the same viewing conditions and to transformed objects. In the first experiment in this series, we used faces. Figure 5 illustrates the images used. Numbers at the bottom of the figure indicate the dissimilarity index (see the Experimental Procedures), a measure of the changes in the retinal image caused by changing the viewing conditions of the same object or by presenting different exemplars of the same category. Note that dissimilarity produced by translation is the largest, while images of different faces under the same viewing conditions are most similar.

To control for attention or ordering effects, we modified the experimental paradigm. Instead of covertly naming the images, subjects (14) were instructed to perform a one-back recognition task while fixating, namely to notice whether consecutive images belonged to the same individual or to different individuals. Furthermore, each condition was shortened and repeated three times in random order, using different images; consecutive face epochs contained images of different individuals (see the Experimental Procedures for details).

LOC was defined by a statistical test that searched for voxels activated preferentially by different faces compared to highly scrambled images (different > scrambled, other conditions ignored). An example of the activation map in one subject is shown in Figure 6a. LOC voxels were maximally activated by images of different

individuals photographed in the same viewing conditions (different) and least activated by highly scrambled images (scrambled). Similar to the previous experiments, LOC voxels showed a signal reduction when identical face images were presented (Identical, $0.94\% \pm 0.20\%$ signal change, compared to Different, $1.84\% \pm 0.18\%$; adaptation ratio, 0.60 ± 0.07).

As described previously (Malach et al., 1995; Grill-Spector et al., 1998a), LOC is a large complex (red contour in Figure 6c) that can be roughly described by three vertices: dorsal, posterior, and anterior. Table 1 provides the Talairach coordinates of these three vertices. These values are within ± 8 mm of the range of LOC coordinates described in our previous studies (Grill-Spector et al., 1998a).

The more advanced design of face experiment 1 allowed us to search for functional differences between various parts within the LOC. A voxel by voxel analysis indeed revealed a consistent difference between two LOC subregions. Specifically, LOC voxels were defined by the test: different faces > scrambled (other conditions ignored). They were then separated into two subdivisions based on anatomical and meridian mapping criteria. The caudal-dorsal subdivision was located consistently lateral to a lower meridian representation on the lateral aspect of the occipital lobe (middle cyan contour marked by an arrow in Figure 6b). It was situated lateral and posterior to MT, extending into the posterior inferior-temporal sulcus (see Figure 6c). The anterior-ventral subdivision (PF/LOa, yellow arrows in Figure 6a and LOa in Figure 6c) was located within the fusiform gyrus anterior to areas V4/V8, extending into the occipitotemporal sulcus. Note that this partition of the LOC was based on meridian mapping and anatomical cues that were unrelated to the issue of adaptation. Nevertheless, a substantial difference in the functional profiles was revealed when these subregions were analyzed separately.

The results of the separate analysis of the two subdivisions are shown in Figure 7a (time courses) and Figure 7b (adaptation ratios). Both regions were maximally activated by images of different individuals (Diff in Figure 7a) and were adapted by repeated presentation of identical images (Ident in Figure 7a). However, there was a difference between the two subdivisions in their recovery from adaptation, mainly in the object translation epochs. While the caudal-dorsal LO voxels (Figure 7b, red) exhibited almost complete recovery from adaptation (ratio, 0.94 ± 0.17), anterior-ventral PF/LOa voxels (Figure 7b, yellow) showed only partial recovery under object translation (ratio, 0.74 ± 0.08). We tested the significance of the adaptation effects across the group. The ratios that were statistically significant ($p < 0.01$) are denoted by asterisks in Figure 7 and Figure 8. Note that PF/LOa was significantly adapted by translations of the same face (see Figure 7b), but the slight adaptation of LO did not reach a statistically significant level.

To confirm the functional differentiation between LO

(c) Averaged time courses ($n = 7$) obtained from the object-related regions highlighted by the Kolmogorov-Smirnov statistical test: Lg and Sm and Sc > N and T. Presentation format as in Figure 3. Abbreviations are the same as in (a). Note the gradual adaptation in the identical epoch. Changing the image size (Sz) did not remove the adaptation effect.

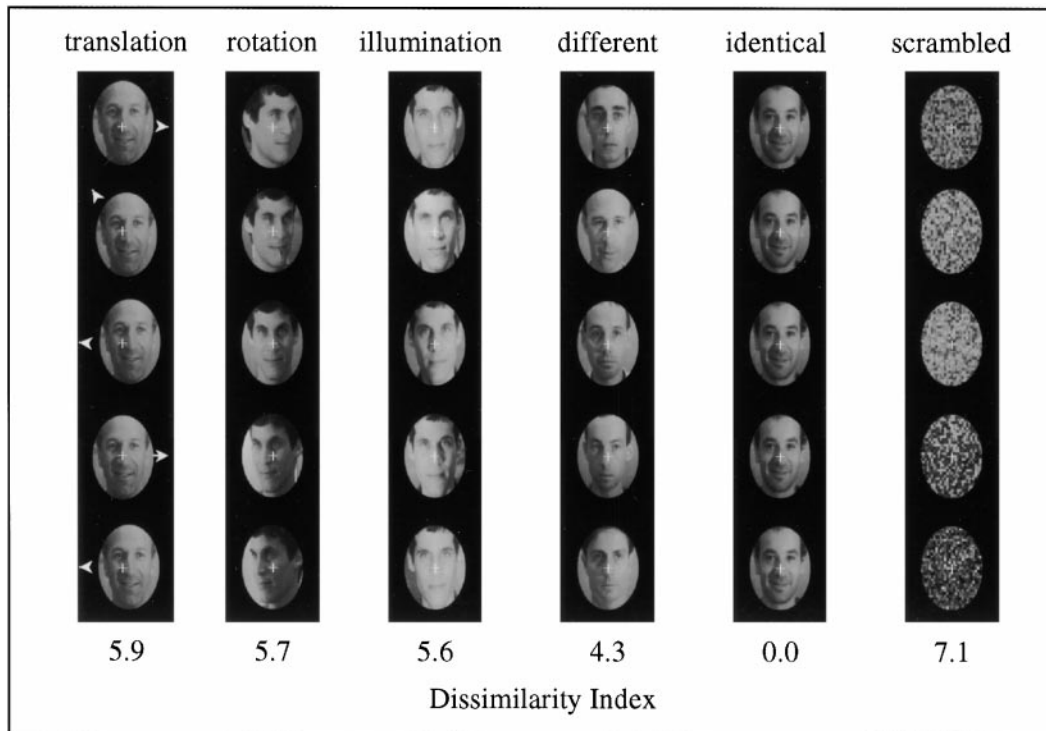


Figure 5. Face Experiment 1: Translation-Illumination-Rotation Invariance

Examples of images presented in the various conditions are shown in columns (see the Experimental Procedures). Translation indicates the same face translated in the image plane. Rotation is the same face rotated around vertical axis. Illumination is the same face illuminated from five directions. Different is five individuals shown in the same viewing conditions. Identical indicates five repetitions of an identical face. Scrambled stands for five highly scrambled faces. Numbers indicate the average retinal dissimilarity between images in an epoch. Note that translation, rotation, and illumination dissimilarity were greater than different face dissimilarity.

and PF/LOa, we tested whether PF/LOa was significantly more adapted by translations compared to LO. This test, performed for all face experiments, revealed that the difference was statistically significant ($p < 0.001$, paired t test, $n = 20$).

Interestingly, even PF/LOa voxels that exhibited the highest degree of adaptation largely recovered from adaptation when the viewpoint or the direction of illumination of the same face changed (ratios, 0.88 ± 0.10 and 0.87 ± 0.13 , respectively). To evaluate the differential nature of adaptation within PF/LOa (i.e., the stronger adaptation by translation compared to illumination and rotation), we calculated, for each subject, the following activation ratios: translation/rotation and translation/illumination. We then tested whether these ratios were significantly smaller than 1.0. The results for both ratios were significant (translation/rotation < 1.0 , $p < 0.03$, $n = 14$; translation/illumination < 1.0 , $p < 0.02$, $n = 14$). However, it should be noted that there was some variability between subjects: in two out of the fourteen subjects, there was a less pronounced differential effect in PF/LOa.

To exclude the possibility that the adaptation in translation epochs was due to eye movements, we measured eye movements in four subjects who participated in two or more fMRI scanning sessions (see the Experimental Procedures). Overall, subjects were able to maintain stable fixation during each epoch. The range of saccades around the fixation point accumulated during the

whole duration of the longest experiment (8 min) was 2° ; occasionally (once or twice during an experiment), subjects made a larger saccade, but it was never larger than 3° of visual angle. Note that the range of translations of the face around fixation was 5.625° and that the subjects were able to maintain stable fixation within each 10 s epoch. Thus, it is highly unlikely that the source of adaptation was tracking eye movements.

Face Experiment 2: Size-Translation-Rotation Invariance

To compare the fMR-A to size with respect to the other transformations, we conducted face experiment 2 (see the Experimental Procedures), which examined the effects of three transformations: size, translation, and rotation. Each transformation occurred twice, once before the corresponding adapting epoch and once after it. Presentations of the same face were separated by at least seven epochs (1 min 38 s).

The experiment was performed on nine subjects. The functional maps derived by the test (faces > textures) were similar to face experiment 1 and are not shown. Time courses averaged across repetitions, and subjects are depicted in Figure 7c, and adaptation ratios are given in Figure 7d. Similar to face experiment 1, the results revealed a differential adaptation profile in the LOC. The time course and adaptation ratio were extracted separately from each subdivision (LO, PF/LOa). The caudal-dorsal region (LO; Figures 7c and 7d, red)

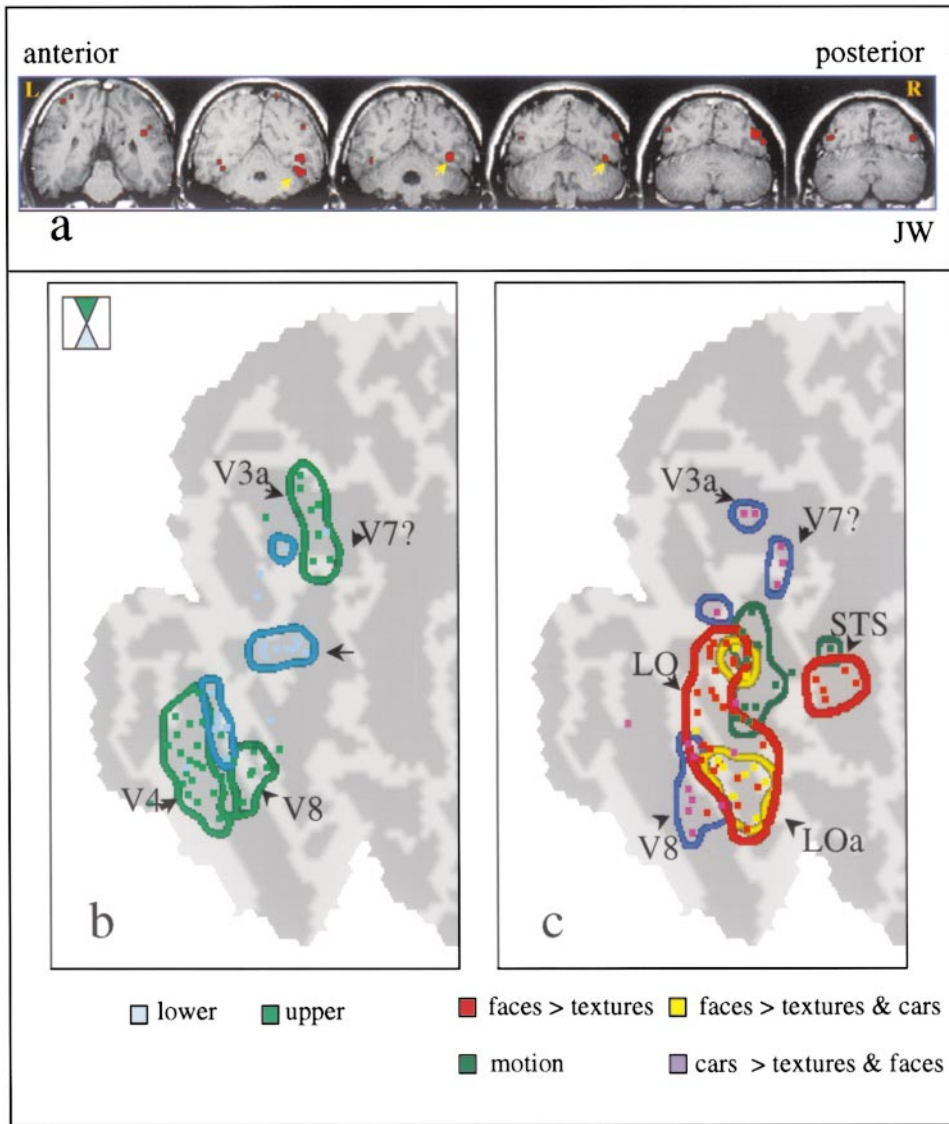


Figure 6. Face Experiment 1: Activation Maps

(a) Six consecutive oblique sections taken from one subject. Same conventions as in Figure 2a. Preferential activation to faces (see Figure 5) is depicted in red and corresponds to the LOC. Statistical test: different faces > scrambled, $p < 0.001$. Yellow arrows indicate PF/LOa.
 (b) Flattened cortical representation of the lower and upper vertical meridians in V4, V3a, and V8 in the right hemisphere. The Talairach coordinates of these meridians (four subjects; see Table 1) were projected onto a flattened representation. Each point corresponds to a specific focus taken from a subject; boundaries indicate the estimated intersubject variability. Cyan, lower vertical meridian; green, upper vertical meridian. The arrow indicates a lower meridian representation near LO.
 (c) Flattened map of shape selective regions in the right hemisphere, same subjects and methods as in (b). Red, regions preferentially activated by faces (test: faces > scrambled); yellow, most specific face voxels (faces > cars and scrambled) in the face and car experiment; purple, car voxels (cars > faces and scrambled). Note that voxels that were activated by faces compared to scrambled (red) were found in LO, PF/LOa, and STS. In the ventral cortex, there was some segregation to voxels that preferred faces (yellow) and cars (purple). Car-selective regions largely overlapped retinotopic areas.

showed substantial recovery from adaptation induced by size, translation, and rotation. In the anterior–ventral part (LOa; Figures 7c and 7d, yellow), there was again a marked difference between viewing conditions with strongest adaptation during position and size changes and only slight adaptation for rotations of the same face. The differential profile of adaptation was statistically significant (translation/rotation < 1.0 , $p < 0.01$, $n = 9$; size/rotation < 1.0 , $p < 0.04$, $n = 9$).

In face experiment 2, there was some variability between subjects in the level of recovery from adaptation. In three out of nine subjects, LO voxels were also largely adapted during the translation and size epochs. In one subject, there was no adaptation for any of the image transformations even in PF/LOa.

The Face and Car Experiment

It could be argued that the adaptation effects revealed in the face experiments are unique to this category,

Table 1. Talairach Coordinates

	Left			Right		
	X	Y	Z	X	Y	Z
LO	-41 ± 5mm	-77 ± 6mm	3 ± 7mm	40 ± 6mm	-72 ± 7mm	2 ± 5mm
	-36 ± 7mm	-71 ± 7mm	-13 ± 5mm	37 ± 5mm	-69 ± 7mm	-10 ± 4mm
PF/LO _a	-38 ± 5mm	-50 ± 6mm	-17 ± 5mm	33 ± 4mm	-47 ± 6mm	-14 ± 4mm

Talairach coordinates (Talairach and Tournoux, 1988) of four subjects whose individual foci are depicted in Figure 6c. They were derived from regions located lateral to retinotopic areas V4/V8 that showed significant preference for objects compared to noise patterns in the face and face and car experiments (see red contour in Figure 6c). The LO complex can be described by three vertices: the first row corresponds to the dorsal posterior vertex, the second to the ventral posterior vertex, and the third to the ventral anterior vertex. The first two vertices bound LO, and the third vertex defined the center of PF/LO_a in Talairach space. Values represent the mean ± standard deviation in mm.

since faces are widely considered as a special class of objects (Valentine, 1988; Farah et al., 1995, 1998; Kanwisher et al., 1997). To examine this point, we conducted a face and car experiment that compared, in six subjects, the fMR-A effect for two object categories, faces and cars, under two image transformations, rotations and translations. As before, activation during these transformations was compared to epochs in which different exemplars of the same category were shown. Figure 8a depicts the images shown in each epoch (see the Experimental Procedures). As in the previous experiments, a dissimilarity index was calculated and is shown at the bottom of Figure 8a. We ran a statistical test that searched for voxels that were activated preferentially by different faces and cars compared to scrambled images; other epochs were ignored in this test (different faces and different cars > scrambled). As in the face experiments, we found differential fMR-A for the different transformations both for faces and cars. We separated the LOC into the two subdivisions (LO and PF/LO_a) using anatomical and meridian mapping landmarks. The activation profiles and the adaptation ratios are shown in Figures 8b and 8c for caudal-dorsal LO and in Figures 8d and 8e for anterior-ventral PF/LO_a. In both subdivisions, the absolute level of the fMR signal was higher for faces compared to cars (see Figures 8b and 8d), although faces and cars were given the same weight in the statistical test. Interestingly, despite this difference, the level of fMR-A was similar for faces (orange in Figure 8c) and cars (blue in Figure 8c). In caudal-dorsal LO, rotations caused a recovery from adaptation (i.e., an elevated signal compared to epochs of identical images). However, in this experiment, a smaller degree of recovery from adaptation was detected in LO in the face translation epochs.

Similar to the previous experiments, PF/LO_a exhibited a somewhat deeper fMR-A both for faces (orange in Figure 8e) and cars (blue in Figure 8e). Inspecting the time course of activation showed that PF/LO_a voxels were substantially adapted when the same object was translated, regardless of object class. These voxels were less adapted by rotated versions of the same object (see Figure 8e). Notice that despite the substantial difference in the absolute level of activation produced by the two object categories (Figure 8d), the level of adaptation was quite similar regardless of object class. The significance of the differential profile of the fMR-A was verified (translations/rotations < 1.0, p < 0.01, n = 6, both object classes).

We also searched for subregions that were specifically activated either by faces (faces > cars and scrambled) or by cars (cars > faces and scrambled). The first

test revealed that a portion of PF/LO_a was most selective to faces compared to cars. This region is illustrated in Figure 6c by the yellow contour and could possibly correspond to the fusiform face area FFA (Kanwisher et al., 1997). Car-selective voxels (purple in Figure 6c) were found in dorsal areas (V3a, V7?; Tootell et al., 1998b) and in the collateral sulcus (V4/V8). The majority of these voxels (purple contour in Figure 6c) overlapped with regions that show some degree of retinotopy (V3a, V4/V8). A small number of voxels that showed preferential activation to cars were also found in LO and PF/LO_a.

Discussion

The Nature of the fMR-A

The fMR-A described in this study was a consistent phenomenon that appeared in all subjects and under a variety of stimulus conditions. However, the magnitude of the effect varied between experiments, suggesting that additional factors modulated the strength of the adaptation effect. Likely factors were the duration of the adaptation period (longer epochs produced deeper adaptation), the type of stimuli, and the order of the different epochs.

fMR-A provides another defining characteristic of the LO complex: more medial, primary visual areas appear to be less affected than LOC (Figure 3a), while area V4 showed an intermediate functional profile. Such adaptation effects may be a unique feature of high-level object-related areas. Alternatively, it may be that the specific object stimuli presented or the brief flicker introduced at the end of each image presentation were an ineffective stimulus for adaptation in primary areas. It should be noted that under different stimulus conditions adaptation was observed in V1 (Tootell et al., 1998a).

The adaptation was typically rapid, occurring within the first few seconds of presentation so that the fMR signal never attained the nonadapted level. Additionally, a more gradual reduction in signal amplitude was also observed, particularly in cases of partial adaptation (e.g., Figure 3c, epoch 2, Figure 4c, and Figure 7c).

The fMR-A was strongest when an identical object image was repeatedly presented for an extended period and declined as the separation between repetitions was increased (Figure 3e). It should be noted that in the adaptation-duration experiment, both the time and number of different intervening pictures were changed concurrently. Consequently, the possibility that an increasing number of intervening pictures gradually eliminated the adaptation effect cannot be ruled out at this point.

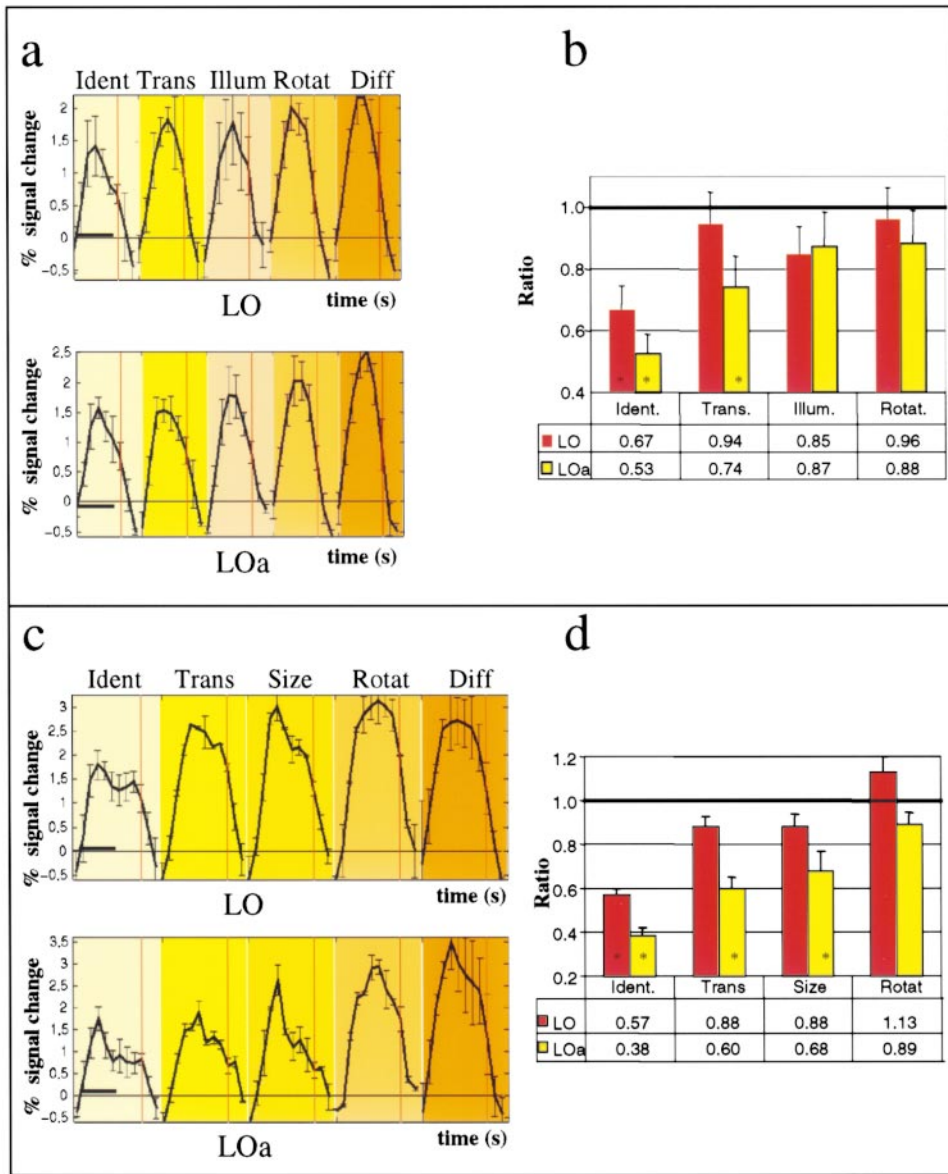


Figure 7. Face Experiments: Time Courses and Ratios

- (a) Face experiment 1 time courses taken separately from LO and PF/LOa and averaged across 14 subjects and 20 scans (three versions of the experiment; see the Experimental Procedures). Recurrences of the same condition were averaged; error bars indicate the standard deviation of a condition. Percent signal change was measured from the adjacent epochs. The dark horizontal bar equals 10 s. Red vertical line indicates the termination of the visual stimulation in an epoch. Abbreviations correspond to epochs shown in Figure 5.
- (b) Face experiment 1 adaptation ratios calculated as the mean signal in an epoch divided by the mean signal in the different epoch. A ratio of 1.0 indicates no adaptation. Ratios that were significantly less than 1.0 are marked by asterisks. Error bars indicated 1 SEM. Note the difference in the ratios in LO and PF/LOa in the translation epoch.
- (c) Face experiment 2 time courses taken separately from LO and PF/LOa averaged across nine subjects. Conventions and abbreviations are the same as in (a). The time scale is the same as in (a), but epochs were longer in this experiment. Note the similar sensitivity to translation and size changes.
- (d) Face experiment 2 adaptation ratios calculated for nine subjects. Conventions are the same as in (b).

Neuronal Mechanisms Underlying the Adaptation Effect

A straightforward neuronal explanation for the fMR-A effect is a reduction in neuronal activity. Neuronal adaptation effects were found in monkey IT, where repeated presentation of the same stimulus resulted in a decreased activation of neurons, a phenomenon termed "adaptive mnemonic filtering" (Miller et al., 1991). This effect has interesting parallels with the fMR-A reported

here, in particular a gradual increase of adaptation level with increased repetition rate (Li et al., 1993).

However, we emphasize that at this stage other potential sources for adaptation-like effects in the fMR signal cannot be excluded. One alternative may be that in the nonadapting epochs, distinct neuronal groups selective for different shapes were sequentially activated. If the activity of each neuronal group or its effect on the hemodynamic response lasted beyond the termination of the

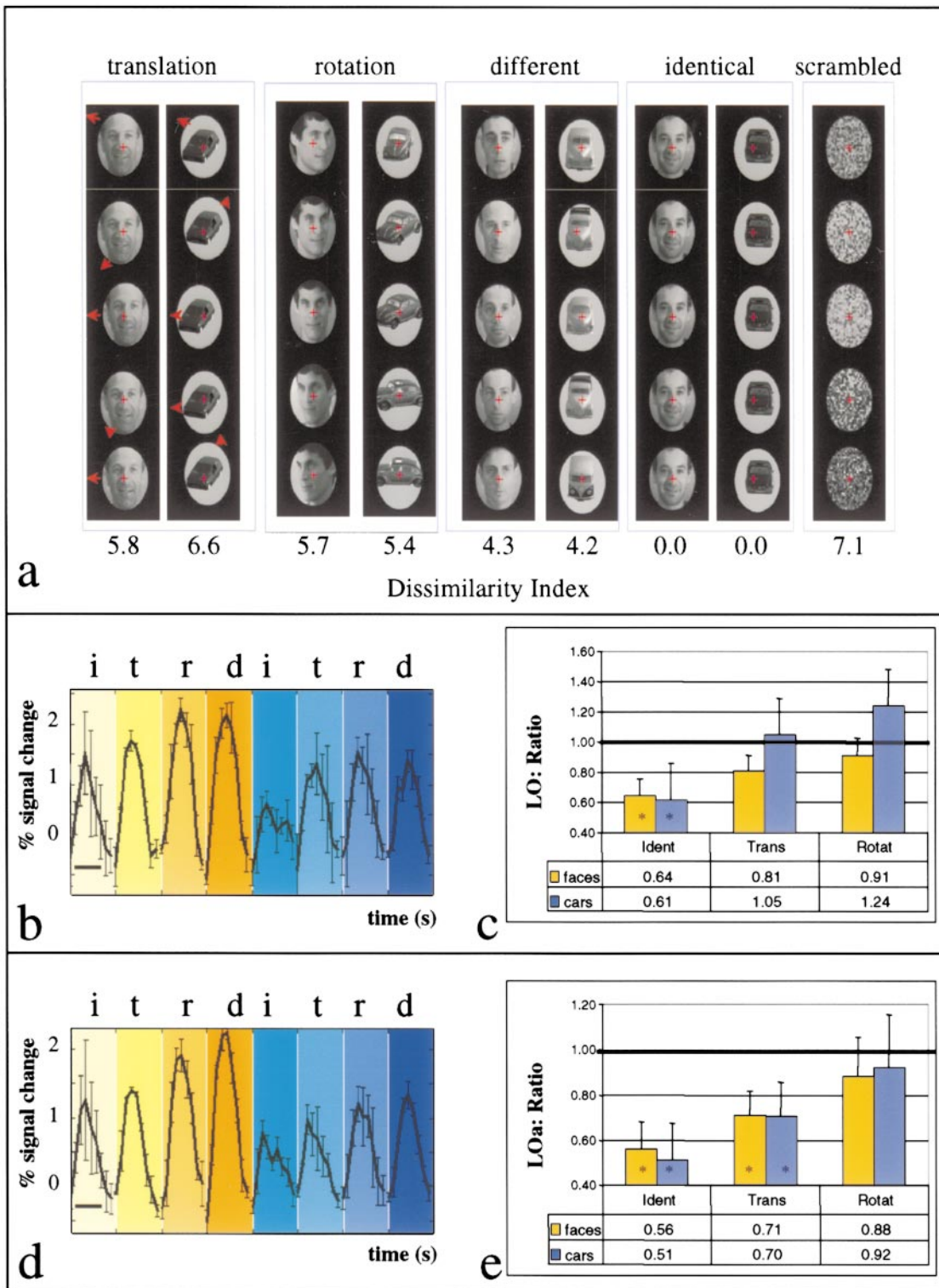


Figure 8. Face and Car Experiment

(a) Examples of images presented in the various conditions are shown in columns (see the Experimental Procedures). Translation indicates five instances of the object translated in the image plane. Rotation indicated five views of the same object. Different denotes five different views of the same object. Identical indicates five repetitions of an identical image. Scrambled denotes five highly scrambled object images. Numbers at bottom indicate the average dissimilarity between images in a condition. Note that translation dissimilarity is greater than different face dissimilarity.

(b-d) Time course and adaptation ratios of LOC voxels activated preferentially by objects (faces and cars > scrambled). The LOC was subdivided into LO and PF/LOa using meridian mapping and anatomical criteria.

optimal stimulus for that group, an accumulation of activation causing a gradual buildup of the fMR signal could have occurred, while in the adaptation epochs, only a single population of shape-selective neurons was continuously activated, leading to a reduced signal. It should be noted that an event-related fMRI study (Buckner et al., 1998) reported a somewhat similar adaptation effect following single exposure to object pictures. This argues against a buildup mechanism being a full explanation of the fMR-A phenomenon.

Top-Down or Feed-Forward Adaptation?

The neuronal adaptation in IT neurons has a relatively short latency that makes the involvement of feedback from higher cortical structures unlikely (Lueschow et al., 1994). The temporal dynamics of the human adaptation effect are not known yet, so the analogy to monkey IT remains to be demonstrated, perhaps using ERP measurements (Rugg et al., 1995).

The differential adaptation profile in LOC subregions is incompatible with a global, nonspecific arousal being the source of the effect. The strong activation caused by different exemplars of the same semantic category (e.g., faces, cars) makes it less likely that an abstract semantic representation produces the adaptation via top-down control. The stronger fMR-A produced by some image transformations compared to others further suggests that this is not a general arousal effect.

Subdivisions of the LOC

In the original description of LOC (Malach et al., 1995), it was suggested that this large cortical region is likely to be a complex of several areas. Indeed, the present fMR-A results revealed at least two putative subdivisions within this complex, which exhibited somewhat different adaptation profiles. The LOC was defined functionally as a region that preferentially activates to objects but not to textures (Malach et al., 1995; Grill-Spector et al., 1998a, 1998b; see Figures 3c and 4c). This shape selectivity was observed both for caudal-dorsal LO and anterior-ventral PF/LOa (see Diff in Figures 7a and 7c). Moreover, both regions were significantly adapted by repeated presentation of identical images (e.g., Figures 7b and 7d). However, a consistent difference between these areas was observed in their sensitivity to position and size changes that produced less adaptation in LO compared to PF/LOa. Hence, PF/LOa was more invariant to changes in the object's position in the visual field compared to LO.

It was found in previous studies that LOC activation does not change significantly with substantial changes in visual field position (Grill-Spector et al., 1998a, 1998b) or with changes of up to 4-fold in object size (Malach et al., 1995). However, as pointed out in the introduction,

such apparent "invariance" may be the consequence of measuring overall fMRI signal produced by a heterogeneous mixture of highly selective groups of neurons. The use of the fMR-A effect enabled us to distinguish between voxels that contain neurons that are truly translation invariant (in PF/LOa) and voxels that contain a mixture of position-sensitive neurons in a region that as a whole does not manifest clear retinotopy (LO).

The fact that LO voxels show some sensitivity to position and size changes also corresponds to the finding that these voxels were located near a region that shows some retinotopy (lower visual field representation; see Figure 6b). A region similar to LO was reported by Tootell et al. (1998b) to contain a foveal-peripheral differentiation.

Additional support for the subdivision reported here comes from Halgren et al. (1999), who identified two face-responsive regions: LO located dorsally and posterior fusiform (PF) area, located ventrally. The latter showed a higher degree of selectivity to faces and presumably corresponds to the region within PF/LOa that showed a higher degree of face selectivity in the face and car experiment (see Figure 6c, yellow contour).

The partition of the LOC, which is shape selective, into posterior and anterior regions, with the posterior being more sensitive to object transformations, is also consistent with several lesion studies. Damage to areas V4 and posterior IT (Weiskrantz, 1990; Schiller, 1995) appears to affect the ability to compensate for object transformations such as size (Humphrey and Weiskrantz, 1969; Ungerleider et al., 1977), orientation, and illumination (Weiskrantz and Saunders, 1984), rather than the ability to recognize nontransformed shapes. In contrast, lesions to anterior IT caused a general deterioration in recognition capacity (Weiskrantz, 1990). Evidence from priming studies also shows that in some conditions priming is sensitive to the location of the object in the primed condition (Edelman and Newell, 1998; Bar and Biederman, 1999).

Differential Invariance in LOC

This study revealed that different image transformations produce different levels of adaptation within PF/LOa. Adaptation in PF/LOa was found to be more invariant to size and position compared to illumination and viewpoint. Note that a similar trend was also observed in LO, although it was quantitatively weaker. These neuronal invariances should be contrasted with the high degree of shape selectivity in PF/LOa revealed by the lack of adaptation in the differently shaped objects epochs. The marked differences in adaptation levels cannot be explained by the raw physical similarity of object images. Pixel-wise Euclidean distance measures of the similarity

(b) LO time course ($n = 6$). Conventions are the same as in Figure 7a. Face epochs are colored yellow-orange, and car epochs are colored blue. i, identical; t, translation; r, rotation; d, different.

(c) The adaptation ratio of LO voxels (same conventions as in Figure 7b). Ratios were calculated separately for faces (orange) and cars (blue). Note that no adaptation equals a ratio of 1.0. Asterisks indicate significant reduction.

(d) PF/LOa time course ($n = 6$) is the same conventions as in (b).

(e) The adaptation ratio of PF/LOa voxels, with the same conventions as in (c). Note that both for cars (blue) and faces (orange), there is larger adaptation by translation compared to rotation.

between object pictures (see the Experimental Procedures) show that the different pictures of the same semantic category taken under the same viewing conditions were in fact more similar to each other physically (i.e., as retinal images) than the pictures in the size and translation epochs that produced adaptation. These results are in line with the reports of translation and size invariance in macaque IT by several research groups (Gross et al., 1972; Ito et al., 1995). Indeed, Lueschow and colleagues (1994) have used the neuronal adaptation phenomenon to quantitate size and translation invariance of IT neurons.

The adaptation paradigm used here has some commonalities with the phenomenon of visual "priming" in which repeated presentation of visual stimuli changes the subject's performance (Schacter and Buckner, 1998; Wiggs and Martin, 1998). Some of the priming studies show size and position invariance (Biederman and Cooper, 1991; Fiser and Biederman, 1995; Wiggs and Martin, 1998); in others, the invariance is incomplete (e.g., Dill and Edelman, 1997).

In our experiments, PF/LOa showed sensitivity to different views of the same objects. This is consistent with physiological findings. Neurons in anterior IT are sensitive to specific views of faces (Perret et al., 1985; Logothetis and Sheinberg, 1996; Wang et al., 1996) and views of novel objects (Logothetis et al., 1995). Even voxels that showed the highest degree of face selectivity recovered from adaptation when the same face was rotated. This indicates that the representation of a face, at least at the level of PF/LOa, is not viewpoint invariant, arguing against a full 3D object-centered representation as proposed by some theories.

One surprising result was that viewing the same object under different directions of illumination resulted in substantial recovery from adaptation. Several models suggest that extraction of illumination could be done by lower visual areas (e.g., Lehky and Sejnowski, 1988). Our results suggest that sensitivity to the direction of illumination is retained even in higher levels of the visual hierarchy. While size and position changes are probably compensated for in PF/LOa, illumination is not. These results are in line with the reported sensitivity of IT neurons to stimulus shading (Ito et al., 1994). Recent psychophysical experiments (Tarr et al., 1998) show the importance of illumination in object recognition tasks and suggest that illumination effects serve to remove 3D ambiguities.

Representation of Various Object Categories within the LOC

It is still a matter of debate whether faces are a special object category (Kanwisher et al., 1997; Farah et al., 1998) or whether they are treated like other object classes (Tovée, 1998). We investigated this issue by examining how the same image transformations are represented in the brain for faces and for cars. The absolute signal for faces was higher in LOC voxels compared to cars (see Figures 8b and 8d). However, adaptation level and the treatment of translation and viewpoint were fairly similar for both object categories (see Figures 8c and 8e). Both faces and cars produced more adaptation for translation compared to viewpoint (see Figures 8c

and 8e). This indicates that the underlying substrate for representing different objects is similar, in that there is higher degree of translation invariance compared to viewpoint invariance.

We also found that face-selective voxels were largely segregated from car-selective ones. The location of most car-selective voxels in mildly retinotopic areas suggests that the preferential car activation in these voxels is due to the statistics of low-level features in the car images and does not reflect some aspect of semantic mapping. However, a separate group of more anterior voxels in largely nonretinotopic, ventral cortex indeed showed consistent preference for cars compared to faces and was usually located in the collateral sulcus, medial to face selective regions. The potential relation of this modularity in ventral cortex to feature-based representations remains to be studied.

The Source of the Preferential Face Activation in the LOC

The results of these adaptation experiments may provide a clue to the source of higher activation by faces compared to cars in the LO complex. Two possible sources for such preferential activation can be envisioned. One possibility is that the LOC contains a heterogeneous collection of neurons, including some highly face-selective and car-selective neurons, with the former outnumbering the latter. Because the fMRI signal is an average of the entire neuronal population, such an uneven representation would lead to stronger activation by faces. An alternative possibility is that the entire neuronal population in the LOC is activated preferentially to faces, but the neurons are not very selective and are also activated by car images, albeit to a lesser degree.

Our results, which show clear adaptation to car images both in LO and PF/LOa despite the weaker activation to these stimuli, support the former hypothesis (given that IT neurons adapt selectively to their optimal stimulus and do not show a generalized adaptation) (Li et al., 1993). Shape-selective adaptation is also implied by the lack of "semantic" adaptation to different exemplars of the same category (see Figure 4c). If indeed the adaptation in a neuronal population is produced only by the optimal stimuli for that population, one has to conclude that the adaptation to cars observed in the LOC reveals the existence of car-selective neurons within this region.

Adaptation as a Tool for Studying Neuronal Properties

The use of fMR-A need not be limited, in principle, to shape adaptation and invariances and could be readily extended to other neuronal systems in which adaptation is manifested. By manipulating experimental parameters and testing recovery from adaptation, it should be possible to gain insight into the functional properties of cortical neurons that are beyond the spatial resolution limits imposed by fMRI.

Experimental Procedures

The experimental setup and protocols were described in detail elsewhere (Grill-Spector et al., 1998a). We present here a brief account of the main aspects of the experiments.

MRI Setup

Seventeen healthy volunteers (ages 19–47; eight females) who gave written informed consent participated in the study. The Chaim Sheba Medical Center ethics committee approved the experimental protocol. Subjects were scanned in a 1.9 T scanner (whole-body, 2T-Prestige, Elscint, Haifa, Israel) equipped with a birdcage headcoil. Experiments included sagittal localizers, high-resolution (0.8 mm × 1.5 mm × 5 mm) T1 weighted images (see Figure 2a, top), and functional imaging EPI pulse sequences (a T2* weighted multislice gradient echo sequence; TR/TE/Flip angle = 2000/45/90° with FOV 38.4 × 19.2 cm², matrix size = 128 × 72, and in-plane resolution of 3 × 2.7 mm. Slices were oriented perpendicular to the calcarine sulcus. The scanned area included 6–12 slices, 4 or 6 mm thick, that covered most of the occipital lobe, with a slight invasion to the parietal and temporal lobes (see Figure 2a).

Visual Stimulation

Back-projected images were viewed through a tilted mirror providing 40° × 30° of visual angle. Experiments lasted 5:20–8:00 min, divided into 10–30 s long epochs. All experiments included a central (0.3°) fixation cross. Pictures were stationary and achromatic. A 125 ms or 250 ms mean luminance blank was interposed between consecutive images to match the interimage transients in all epochs. Subjects fixated and performed covert naming (adaptation-duration and size invariance experiments) or one-back matching (all other experiments). In addition, we mapped for each subject the visual meridians.

Experiments

Adaptation-Duration Experiment

The adaption-duration experiment (see Figure 1) consisted of five object-containing epochs lasting 32 s alternating with mean luminance blanks, randomly oriented triangles, or highly scrambled pictures. Images were gray level photographs (30° × 30° visual angle) of objects presented for 875 ms interposed with 125 ms blanks. Object categories included animals, faces, and man-made objects. Cycle of different objects ranged from a single object presented repeatedly for 32 times (epoch 1), through cycles of two, four, and eight different objects, and an epoch containing 32 different objects. The time sequence of the epochs is given in Figure 1b.

Size Invariance Experiment

The size invariance experiment consisted of nine 20–30 s epochs (see Figure 4a). Presentation rates were the same as in the adaptation-duration experiment. All object images were achromatic drawings. Epochs included Noise (20 random dot patterns), Identical (a single dog [18° × 18°] presented repeatedly for the entire epoch [30 s]), Texture (same as in the adaptation-duration experiment), Size (same image as in Identical but changed in size in a pseudorandom order over a range of 10°–30°), Semantic control (30 different drawings of dogs [15° × 15°]), Small (30 different common objects [7° × 7°]), and Large (same as in Small but reordered [size, 22° × 22°]).

Face Experiment 1

The experiment 1 contained 32 blocks of five images. Face images (see Moses et al., 1994) of size 9° × 12° alternated with scrambled images or blanks. Each image was presented for 1750 ms followed by 250 ms blank. Epochs included Identical (a single face presented repeatedly), Translation (same face translated over 5.625° around fixation), Illumination (same face illuminated from five different directions), Rotation (same face viewed in five rotations around the vertical axis [-34°, -17°, 0°, 17°, 34°]), Different (five different faces), and Scrambled (face images randomly scrambled into blocks of 10 × 10 pixels). Pixel-wise dissimilarity in the different epoch was the smallest (mean = 4.3) and in the translation epoch, the largest (mean = 5.9; see Figure 5). Each condition was repeated for three times in random order using a different face. Subjects were instructed to perform a one-back matching task while fixating. The experiment was run in three versions (20 scans, 14 subjects) differing in epoch order and face identity.

Face Experiment 2

The experiment contained 29 epochs of 16 images (16.875° × 22.5°) presented for 750 ms + 250 ms blank. Epoch types were Identical, Translation, and Scrambled (same as in face experiment 1). Size

indicates the same face, but changed in size over a range of 9.375° × 14° to 18.75° × 28°. Rotation is the same as in face experiment 1, but rotated over ±90°. Different indicates 16 different faces. Epoch order was balanced. As in face experiment 1, pixel-wise dissimilarity ranking was translation > size = rotation > different. Subjects were required to perform a one-back task via a response box while fixating (same, button 1; different, button 2; blank, alternate buttons). Note that subjects were required to attend changes in all epochs and could not anticipate the epoch order. Thus, for most epochs, the changes in the viewing conditions made the task a nontrivial one.

Face and Car Experiment

The face and car experiment was the same as the face experiment 1 but with the addition of a second object category (see Figure 8a). The experiment consisted of 45 epochs, object epoch alternated with scrambled epochs or blanks. Face and car epochs included translation (two per category), rotation, identical, and different (three per category). Presentation rate was the same as in the face experiment 1. A total of six scans were run.

Mapping Visual Field Meridians

In all of the subjects, the borders of retinotopic visual areas were mapped using two vertical and two horizontal log-polar sections (for details, see Grill-Spector et al., 1998b). This experiment provided an independent and reliable differentiation between the LOC and its neighboring retinotopic visual areas.

Data Analysis

Details are presented in Grill-Spector et al. (1998a). Two scans were rejected due to head motion. First, four image acquisitions were discarded. Images were preprocessed using principal component analysis (Reyment and Jöreskog, 1993; Grill-Spector et al., 1998a). The data of the size invariance experiment were analyzed using Kolmogorov-Smirnov statistical test; data from the adaptation-duration, face experiments, and face and car experiment were analyzed using regression analysis. Activation time courses were obtained from voxels showing highly significant ($p < 0.001$) activation. Statistical maps were spatially smoothed with a 3 × 3 pixel Gaussian filter with a variance of 1 pixel; false positives were verified via a bootstrap method. Note that the conditions tested included only those defining object-related activation (e.g., many > noise) and did not include conditions that were part of the expected outcome.

Percent Signal Change

The percent signal change was calculated as (signal – average signal during baseline epochs)/(average signal during baseline epochs). The baseline was either the blank epochs in the adaptation-duration and size invariance experiments or the adjacent epochs (which were typically scrambled images) in all other experiments.

The Adaptation Ratio

The adaption ratio was defined as the ratio between the activation (percent signal change) in a condition and the activation of the different objects epoch (typically, the maximal, nonadapted epoch). The activation was measured relative to the adjacent (blank or scrambled) epochs to eliminate possible low-frequency fluctuations.

Condition Average Time Courses

All epochs belonging to the same condition were averaged together to provide an average condition epoch time course (e.g., in Figure 7 and Figure 8). Error bars indicate the standard deviation in each time point between reoccurrences of the condition.

Flattened Maps Representation

The Talairach coordinates of foci of interest were calculated for six subjects, who participated in the face and car experiment (Figure 6). These included the lower and upper visual meridian representations, LO voxels, PF/LOa voxels, and face- and car-selective regions. These coordinates were projected via the Caret software (Van Essen and Drury, 1997) onto a standard flattened representation. Figures 6b and 6c show foci whose anatomical position were consistent with the subject's sulcal anatomy. The estimated boundaries indicate the intersubject variability.

Quantitative Analysis of Interpicture Differences

Physical picture similarity within an epoch was calculated as the mean point-wise Euclidean distance between all pairs of pictures

presented in each epoch. Although simple, this analysis provides a baseline for comparison to more sophisticated similarity measures (Moses et al., 1994; Edelman, 1997). Formally, the point-wise distance d_{jk} , is defined by

$$d_{jk} = \frac{1}{n\sqrt{\sum_{x=1}^n [I_j(x) - I_k(x)]^2}} \quad [j, k = 1 \dots p]$$

where n is the number of pixels in an image, $I_j(x)$ is the gray level value of the pixel in location x in the image I_j , and p is the number of images in the epoch. The mean point-wise distance (d) over all images in a condition was calculated as $d = E(d_{jk})$ and taken as the dissimilarity index. The larger this index, the greater the overall physical (i.e., retinal) dissimilarity between all the images in a particular epoch.

Eye Movements Measurement

Eye movements were recorded in four subjects while performing the face and car experiment. The measurements were taken using an infrared eye tracker (Dr. Bouis oculometer). The records were taken outside the magnet, but using identical visual stimuli and task as during the scan.

Acknowledgments

This study was funded by ISF grant 131/97. We thank Y. Moses for providing the face database and E. Sali and A. Zeira for providing the car database. We thank E. Seidemann for assistance in performing the eye movement measurements, E. Okon for technical help and advice, and T. Hendl for helpful comments on the manuscript.

Received March 18, 1999; revised July 27, 1999.

References

- Bar, M., and Biederman, I. (1999). Localizing the cortical region mediating visual awareness of object identity. *Proc. Natl. Acad. Sci. USA* **96**, 1790–1793.
- Biederman, I., and Cooper, E.E. (1991). Evidence for complete translational and reflectional invariance in visual object priming. *Perception* **20**, 585–593.
- Buckner, R.L., Petersen, S.E., Ojemann, J.G., Miezin, F.M., Squire, L.R., and Raichle, M.E. (1995). Functional anatomical studies of explicit and implicit memory retrieval tasks. *J. Neurosci.* **15**, 12–29.
- Buckner, R.L., Goodman, J., Burock, M., Rotte, M., Koutstaal, W., Schacter, D., Rosen, B., and Dale, A.M. (1998). Functional-anatomic correlates of object priming in humans revealed by rapid presentation event-related fMRI. *Neuron* **20**, 285–296.
- Desimone, R., Albright, T.D., Gross, C.G., and Bruce, C. (1984). Stimulus-selective properties of inferior temporal neurons in the macaque. *J. Neurosci.* **4**, 2051–2062.
- DeYoe, E., Carman, G., Bandettini, P.A., Glickman, S., Wieser, J., Cox, R., and Neitz, J. (1996). Mapping striate and extrastriate visual areas in human cerebral cortex. *Proc. Natl. Acad. Sci. USA* **93**, 2382–2386.
- Dill, M., and Edelman, S. (1997). Translation invariance in object recognition, and its relation to other visual transformations. Artificial Intelligence Memo Number 1610. (Cambridge, Massachusetts: Massachusetts Institute of Technology).
- Edelman, S. (1997). Computational theories of object recognition. *Trends Cog. Sci.* **1**, 296–304.
- Edelman, S., and Newell, F.N. (1998). On the representation of object structure in human vision: evidence from differential priming of shape and location. Technical Report, Number 500, University of Sussex, Brighton, United Kingdom.
- Farah, M.J., Klein, K.L., and Levinson, K.L. (1995). Face perception and within-category discrimination in prosopagnosia. *Neuropsychologia* **33**, 661–674.
- Farah, M.J., Wilson, K.D., Drain, M., and Tanaka, J.N. (1998). What is "special" about face perception? *Psychol. Rev.* **105**, 482–498.
- Fiser, J., and Biederman, I. (1995). Size invariance in visual object priming of gray-scale images. *Perception* **24**, 741–748.
- Grill-Spector, K., Kushnir, T., Edmond, S., Itzhak, Y., and Malach, R. (1998a). Cue invariant activation in object-related areas of the human occipital lobe. *Neuron* **21**, 191–202.
- Grill-Spector, K., Kushnir, T., Hendler, T., Edelman, S., Itzhak, Y., and Malach, R. (1998b). A sequence of object processing stages revealed by fMRI in the human occipital lobe. *Hum. Brain Mapp.* **6**, 316–328.
- Grill-Spector, K., Kushnir, T., Edelman, S., Itzhak, Y., and Malach, R. (1998c). Differential processing of faces under various viewing conditions in human lateral occipital complex. Society of Neuroscience 28th Annual Meeting, p. 531.
- Gross, C.G., Rocha, M.C., and Bender, D.B. (1972). Visual properties of neurons in inferotemporal cortex of the Macaque. *J. Neurophysiol.* **35**, 96–111.
- Hadjikhani, N., Liu, A.K., Dale, A.M., Cavanagh, P., Tootell, R.B.H. (1998). Retinotopy and color sensitivity in human visual cortical area V8. *Nat. Neurosci.* **1**, 235–241.
- Halgren, E., Dale, A.M., Sereno, M.I., Tootell, R.B., Marinkovic, K., and Rosen, B.R. (1999). Location of human face-selective cortex with respect to retinotopic areas. *Hum. Brain Mapp.* **7**, 29–37.
- Humphrey, N.K., and Weiskrantz, L. (1969). Size constancy in monkeys with inferotemporal lesions. *Q. J. Exp. Psychol.* **21**, 225–238.
- Ito, M., Fujita, I., Tamura, H., and Tanaka, K. (1994). Processing of contrast polarity of visual images in inferotemporal cortex of the macaque monkey. *Cereb. Cortex* **5**, 499–508.
- Ito, M., Tamura, H., Fujita, I., and Tanaka, K. (1995). Size and position invariance of neuronal responses in monkey inferotemporal cortex. *J. Neurophysiol.* **73**, 218–226.
- Kanwisher, N., Chun, M.M., McDermott, J., and Ledden, P.J. (1996). Functional imagining of human visual recognition. *Brain Res. Cogn. Brain Res.* **5**, 55–67.
- Kanwisher, N., McDermott, J., and Chun, M.M. (1997). The fusiform face area: a module in human extrastriate cortex specialized for face perception. *J. Neurosci.* **17**, 4302–4311.
- Karni, A., Meyer, G., Jezzard, P., Adams, M.M., Turner, R., and Ungerleider, L.G. (1995). Functional MRI evidence for adult motor cortex plasticity during motor skill learning. *Nature* **377**, 155–158.
- Lehky, S.R., and Sejnowski, T.J. (1988). Network model of shape-from-shading: neural function arises from both receptive and projective fields. *Nature* **333**, 452–454.
- Li, L., Miller, E.K., and Desimone, R. (1993). The representation of stimulus familiarity in anterior inferior temporal cortex. *J. Neurophysiol.* **69**, 1918–1929.
- Logothetis, N.K., and Sheinberg, D.L. (1996). Visual object recognition. *Annu. Rev. Neurosci.* **19**, 577–621.
- Logothetis, N.K., Pauls, J., and Poggio, T. (1995). Shape representation in the inferior temporal cortex of monkeys. *Curr. Biol.* **5**, 552–563.
- Lueschow, A., Miller, E.K., and Desimone, R. (1994). Inferior temporal mechanisms for invariant object recognition. *Cereb. Cortex* **4**, 523–531.
- Malach, R., Reppas, J.B., Benson, R., Kwong, K.K., Jiang, H., Kennedy, W.A., Ledden, P.J., Brady, T.J., Rosen, B.R., and Tootell, R.B.H. (1995). Object-related activity revealed by functional magnetic resonance imaging in human occipital cortex. *Proc. Natl. Acad. Sci. USA* **92**, 8135–8139.
- Malach, R., Grill-Spector, K., Kushnir, T., Edelman, G.M., and Itzhak, Y. (1998). Rapid shape adaptation reveals position and size invariance in the object-related lateral occipital (LO) complex. *Neuroimage* **7**, S43.
- Martin, A., Lalonde, F.M., Wiggs, C.L., Weisberg, J., Ungerleider, L.G., and Haxby, J.V. (1995). Repeated presentation of objects reduces activity in ventral occipitotemporal cortex: a fMRI study of repetition priming. *Soc. Neurosci. Abst.* **21**, 1497.
- Miller, E.K., Li, L., and Desimone, R. (1991). A neural mechanism for working and recognition memory in inferior temporal cortex. *Science* **254**, 1377–1379.
- Moses, Y., Adini, Y., and Ullman, S. (1994). Face recognition: the

- problem of compensating for illumination changes. Proceedings of the European Conference on Computer Vision, 286–296.
- Perret, D.I., Smith, P.A.J., Potter, D.D., Mistlin, A.J., Head, A.S., Milner, A.D., and Jeeves, M.A. (1985). Visual cells in the temporal cortex sensitive to face view and gaze direction. *Proc. R. Soc. Lond. B* 223, 293–317.
- Reyment, R., and Jöreskog, K. (1993). Applied Factor Analysis in the Natural Sciences (Cambridge, MA: Cambridge University Press).
- Rolls, E.T., Baylis, G.C., Hasselmo, M.E., and Nalwa, V. (1989). The effect of learning on the face selective responses of neurons in the cortex in the superior temporal sulcus of the monkey. *Exp. Brain Res.* 76, 153–164.
- Rugg, M.D., Soardi, M., and Doyle, M.C. (1995). Modulation of event-related potentials by the repetition of drawings of novel objects. *Brain Res. Cogn. Brain Res.* 3, 17–24.
- Schiller, P.H. (1995). Effects of lesions in visual cortical area V4 on the recognition of transformed objects. *Nature* 376, 342–344.
- Schacter, D.L., and Buckner, R.L. (1998). Priming and the brain. *Neuron* 20, 185–195.
- Sereno, M.I., McDonald, C.T., and Allman, J.M. (1994). Analysis of retinotopic maps in extrastriate cortex. *Cereb. Cortex* 4, 601–620.
- Sobotka, S., and Ringo, J.L. (1993). Investigation of long-term recognition and association memory in unit responses from inferotemporal cortex. *Exp. Brain Res.* 96, 28–38.
- Stern, C.E., Corkin, S., Gonzalez, R.G., Guimaraes, A.R., Baker, J.R., Jennings, P.J., Carr, C.A., Sugiura, R.M., Vedantham, V., and Rosen, B.R. (1996). The hippocampal formation participates in novel picture encoding: evidence from functional magnetic resonance imaging. *Proc. Natl. Acad. Sci. USA* 93, 8660–8665.
- Talairach, J., and Tournoux, P. (1988). Co-Planar Stereotaxic Atlas of the Human Brain (New York: Thieme Medical Publishers).
- Tarr, M.J., Kersten, D., and Bulthoff, H.H. (1998). Why the visual recognition system might encode the effects of illumination. *Vis. Res.* 38, 2259–2276.
- Tootell, R.B., Dale, A.M., Sereno, M.I., and Malach, R. (1996). New images from human visual cortex. *Trends Neurosci.* 19, 481–489.
- Tootell, R.B., Hadjikhani, N.K., Vanduffel, W., Liu, A.K., Sereno, M.I., and Dale, A.M. (1998a). Functional analysis of primary visual cortex (V1) in humans. *Proc. Natl. Acad. Sci. USA* 95, 811–817.
- Tootell, R.B.H., Hadjikhani, N., Mendola, J.D., Marett, S., and Dale, A.M. (1998b). From retinotopy to recognition: fMRI in human visual cortex. *Trends Cog. Sci.* 2, 174–183.
- Tootell, R.B., Mendola, J.D., Hadjikhani, N.K., Liu, A.K., and Dale, A.M. (1998c). The representation of the ipsilateral visual field in human cerebral cortex. *Proc. Natl. Acad. Sci. USA* 95, 818–824.
- Tovée, M.J. (1998). Is face processing special? *Neuron* 21, 1239–1242.
- Ungerleider, L.G., Ganz, L., and Pribram, K.H. (1977). Effects of pulvinar, prestriate and inferotemporal lesions. *Exp. Brain Res.* 27, 251–269.
- Valentine, T. (1988). Upside-down faces: a review of the effect of inversion upon face recognition. *Br. J. Psychol.* 79, 471–491.
- Van Essen, D.C., and Drury, H.A. (1997). Structural and functional analyses of human cerebral cortex using a surface-based atlas. *J. Neurosci.* 17, 7079–7102.
- Wang, G., Tanaka, K., and Tanifuchi, M. (1996). Optical imaging of functional organization in the monkey inferotemporal cortex. *Science* 272, 1665–1668.
- Weiskrantz, L., and Saunders, R.C. (1984). Impairments of visual object transforms in monkeys. *Brain* 107, 1033–1072.
- Weiskrantz, L. (1990). Visual prototypes, memory and the inferotemporal lobe. In *Vision, Memory and the Temporal Lobe*, E. Iwai and M. Mishkin, eds. (New York: Elsevier), pp. 13–28.
- Wiggs, C.L., and Martin, A. (1998). Properties and mechanisms of perceptual priming. *Curr. Opin. Neurobiol.* 8, 227–233.